Journal of Nuclear Materials 390–391 (2009) 544–549

Contents lists available at ScienceDirect

Journal of Nuclear Materials

journal homepage: www.elsevier.com/locate/jnucmat

Measurement of hydrogenic retention and release in molybdenum with the DIONISOS experiment

G.M. Wright [a,*], D.G. Whyte [b], B. Lipschultz [b]

[a] FOM-Institute for Plasma Physics Rijnhuizen, Association Euratom-FOM, A Member of the Trilateral Euregio Cluster, Postbus 1207, 3430 BE, Nieuwegein, The Netherlands
[b] M.I.T. Plasma Science and Fusion Center, 175 Albany St., Cambridge, MA 02139, USA

ARTICLE INFO

PACS:
52.55.Pi
52.40.Hf
28.52.Fa

ABSTRACT

Molybdenum targets are exposed in the DIONISOS experiment to a deuterium (D) plasma ($\Gamma_D \sim 10^{21}$ $m^{-2}\,s^{-1}$) at target biases of 30–350 V and target temperatures of 300–700 K while simultaneously diagnosing the D in the surface with a 3.5 MeV ^{3}He ion beam. The ^{3}He diagnostic beam creates displacements in the Mo lattice which can then trap D, allowing retention far beyond the plasma ion implantation range. The conversion of displacements to trap sites averaged over the ion range is non-linear with a scaling $(\text{dpa})^{\alpha}$, $0.25 \leqslant \alpha \leqslant 0.5$. The beam-induced traps are distributed from the surface to the end of range as opposed to the damage (dpa) profile that is concentrated at the end of range. Measurement of the near-surface D time-dependence has allowed inference of an effective surface recombination rate, which is lower than predicted by theory and at the low end of those found in literature.

1. Introduction

Molybdenum (Mo) is used in several tokamaks (e.g. Alcator C-Mod, TRIAM, FTU) as a plasma-facing component (PFC) material due to its beneficial thermal properties and machinability as compared to tungsten (W). Also like W, both the solubility and inherent trap (sites for H to reside in the material) concentration are very low. It is expected that the hydrogenic retention in Mo will be low. Laboratory results for hydrogenic retention in Mo [1–5] show a low rate of retention when Mo is exposed to H or D ions. However the hydrogenic retention for Mo in a tokamak environment is not well documented. For example, a campaign in Alcator C-Mod was performed with bare Mo PFC (10–15 at.% B on the surface of most tiles). For 10 dedicated discharges, the D retention increased linearly at roughly 1% of incident ion fluence [6,7]. Both the absolute rate of this D retention and the lack of saturation in the Mo PFCs are unexpected. In addition, the hydrogenic retention in a nuclear environment is also not well understood or documented. This becomes a more pertinent and urgent issue as we move towards power producing devices operating in a neutron environment.

The DIONISOS experiment simultaneously exposes the target to a plasma flux and an irradiating MeV ion beam, the latter used for simultaneous analysis of the D content in the sample [8]. This configuration also allows the influence of the plasma and the irradiating ion beam on the hydrogenic retention properties of the Mo targets to be measured independently and synergistically. DIONISOS thus yields insights into how D retention evolves throughout a plasma exposure rather than relying on post-mortem analysis. This reveals insights into the production of trap sites due to material irradiation by MeV-energy ions. The rate of trap production due to the ^{3}He ion beam is related to the rate of lattice damage as measured by displacements per atom (dpa) caused by the impact of the MeV-energy ions.

2. Experiment

The DIONISOS experiment exposes the target to a plasma produced by a helicon RF plasma source, while simultaneously irradiating the surface with a high-energy ion beam produced by a 1.7 MV Pelletron tandem ion accelerator (Fig. 1). In these experiments a 3.5 MeV $^3He^{++}$ beam was used to monitor the D content of the targets with nuclear reaction analysis (NRA) exploiting the ^{3}He(d,p)α nuclear reaction. Further details on the DIONISOS experiment can be found elsewhere [8]. The 3.5 MeV $^3He^{++}$ ions impact the Mo target surfaces at an incident angle of 45° and a scattering angle to the detector of 90°. The typical ion beam spot was circular with a diameter of ~5 mm. The typical ion beam current for the ^{3}He beam was ~1.7 μA for $^3He^{++}$ (0.086 A/m^2). Table 1 lists the beam specifications for each exposure condition utilized in this paper.

The aim of the DIONISOS experiment is to investigate the dynamics of hydrogenic retention by tracking D depth profiles as a function of time. This makes the common method of achieving depth profiles, obtaining energy spectra for several ^{3}He ion ener-

* Corresponding author.
E-mail address: wright@rijnhuizen.nl (G.M. Wright).
URL: http://www.rijnhuizen.nl (G.M. Wright).

0022-3115/$ - see front matter © 2009 Elsevier B.V. All rights reserved.
doi:10.1016/j.jnucmat.2009.01.092

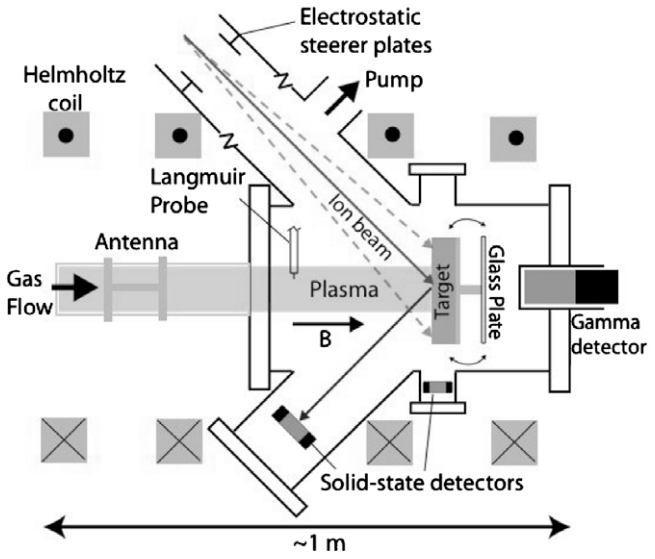

Fig. 1. A schematic drawing of the DIONISOS experiment.

gies [9], unfeasible due to time required to vary the beam energy and collect the data.

For DIONISOS, the D depth profile is obtained using a single ^{3}He energy. Normally a reliable depth profile is not feasible since the solid state detector has a large solid angle and the angular vs. energy distribution becomes convoluted. However, in DIONISOS, the detector is far (~35 cm) removed from the target (to avoid plasma heating) and thus subtends a much smaller solid angle and improves depth resolution of the D profile. The 90° scattering angle for the NRA measurements also helps to broaden the overall energy spectrum and reduce the effect of finite detector energy resolution. The ^{3}He NRA spectra are transformed into D concentration depth profiles using the simNRA program [10,11]. Discrete D and Mo layers in the simulation program produce discrete Gaussian peaks at known energies, based on the depth in the target (Fig. 2). Simulated layers of 500 nm were typically used for the fits in this investigation. Fits began with data from exposures at 300 K where, from the narrow peak in the measured energy spectrum, the D is clearly limited to the first micron. This established the leading edges of the Gaussian curves corresponding to the first micron. For higher target temperatures, as the measured energy spectrum broadened the deeper layers in simNRA were filled in and the surface layer adjusted in magnitude to match the leading edge of the measured spectrum. With He^3 beam currents of ~1.5 μA, spectrum acquisition times (time resolution) can be reduced to 250 s with <10% statistical uncertainties and D sensitivity of ~10 appm.

In these experiments, data was taken at negative target biases of 30, 100, and 350 V with Mo temperatures ranging from 300 to 700 K (see Table 1). The target bias sets the incident ion energies

Table 1
Exposure conditions for Mo targets with voltage biases of 30, 100, and 350 V. The temperature scan is performed in steps of 100 K.

	Target bias		
	30 V	100 V	350 V
Mo Temperature range (K)	300–700	300–700	300–700
Plasma flux density (D/m^2 s)	1.0×10^{21}	1.5×10^{21}	1.0×10^{21}
^{3}He^{++} beam current density (A/m^2)	0.086	0.050	0.086
Exposure time (s)	1500	1000	1500
Plasma fluence (D/m^2)	1.5×10^{24}	1.5×10^{24}	1.5×10^{24}
3.5 MeV ^{3}He^{++} fluence (^{3}He/m^2)	4.0×10^{20}	1.6×10^{20}	4.0×10^{20}

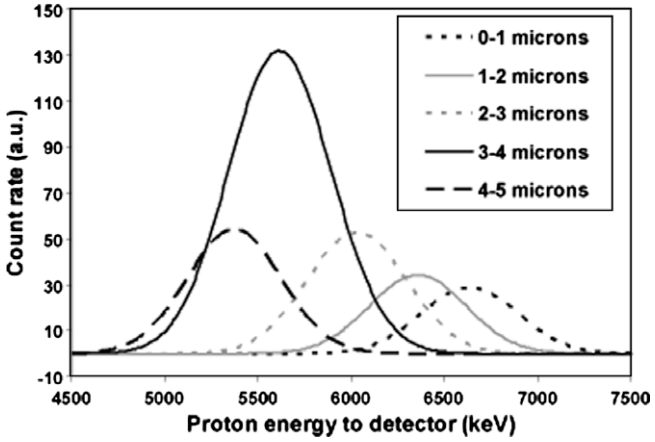

Fig. 2. The Gaussian peaks produced by simNRA for DIONISOS geometry from a series of discrete, 1 μm layers with a concentration of 0.01 D/Mo. The magnitudes of the peaks are determined by the D/Mo ratio in the layer and the energy dependence of the reaction cross-section.

since the electron temperature, T_e, is measured to be 5 ± 1 eV. For the plasma exposures at a constant Mo temperature, the plasma flux density was kept at $1.0 \pm 0.1 \times 10^{21}$ D/m^2 s as measured by a Langmuir probe for all data sets except for the data set at 100 V. For those experiments, the flux density was measured to be $1.5 \pm 0.1 \times 10^{21}$ D/m^2 s (reflection not included). In all cases the to-

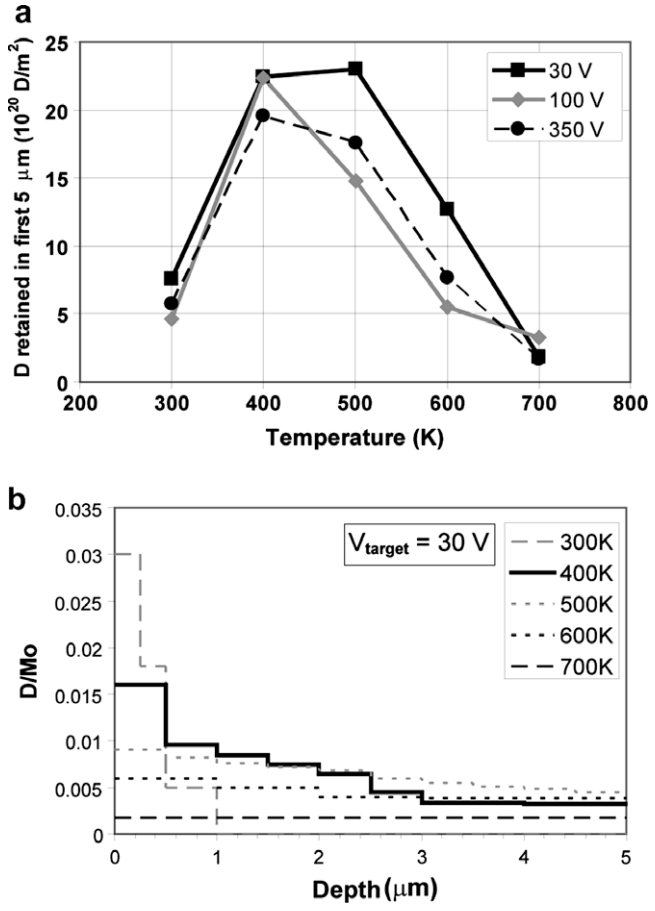

Fig. 3. (a) The measured D retention in the first 5 μm of the ^{3}He-irradiated Mo targets for the various target biases and (b) the corresponding D concentration depth profiles for Mo temperatures ranging from 300 to 700 K at target bias of 30 V. There was no significant variation in profiles due to variations in the target bias.

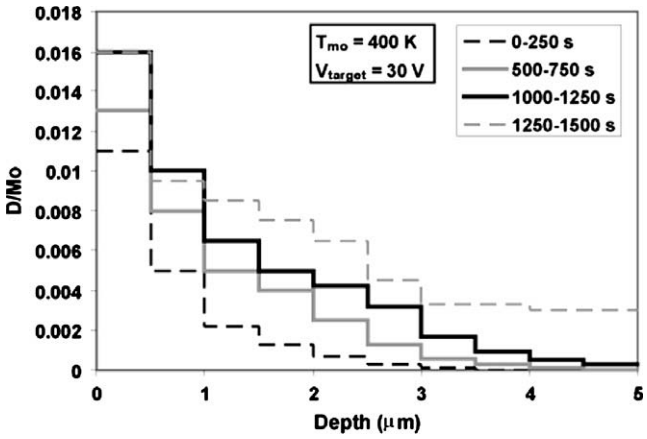

Fig. 4. D depth profiles at various times during a plasma exposure with the ^{3}He ion beam present. Results correspond to the 400 K curve in Fig. 3(b).

tal fluence was kept constant at 1.5×10^{24} D/m^2, corresponding to an exposure time of 1500 or 1000 s depending on the plasma flux density.

The temperature of the target was measured with an ungrounded resistive temperature device (RTD). The surface of the target was also monitored with an infrared camera to ensure there was no deviation from the target temperature due to local heating by the ion beam or plasma. The Mo targets were 99.97% pure Mo plates purchased from Ed Fagan Inc. The targets used in this investigation were purchased in two separate batches. The first batch was used to determine the retention as a function of target temperature and bias (Sections 3.1 and 3.2, Fig. 3) and the second batch was used to determine the influence of the irradiating beam (Section 3.3, Figs. 5 and 6). The targets were exposed in the as received condition with no surface preparation other than cleaning with methanol and a bake at 400 K for ~30 min prior to exposure. Surface roughness was measured to be ~200 nm by interferometry.

3. Results

3.1. D retention as a function of surface temperature and target bias

The results for the total D retention in the first 5 μm (limit of NRA measurement depth) of the surface post-exposure can be seen in Fig. 3(a). The exposure conditions for these targets can be found in Table 1. We note that for real-time D detection the ^{3}He ion beam was irradiating the target throughout these plasma exposures which we will show later has a strong effect on retention. A single target specimen was used for all temperatures for a single target bias. After each plasma exposure the D was thermally desorbed at 750 K until the D concentration, as measured with in-situ with NRA, was <50 appm within the top 5 μm. Since the same specimens were used for all temperatures (but only a single target bias) this introduces the possibility of a history effect. However tests with repeated exposures found these effects to be small, presumably due to the long bake times between exposures. Since the same procedures and sequences were followed for all specimens, any history effects should be minimized for comparative purposes.

The total retention in the first 5 μm increases as the Mo temperature increases from 300 K to 400–500 K (Fig. 3(a)). The corresponding depth profiles of D concentration for the 30 V case are shown for all sample temperatures in Fig. 3(b). There was no significant variation in the D depth profiles due to variations in the target bias. The 600 K and 700 K profiles show a flat or close-to-flat deuterium profile indicating very deep penetration of the D into the surface and/or greater loss of D out the front surface. Since

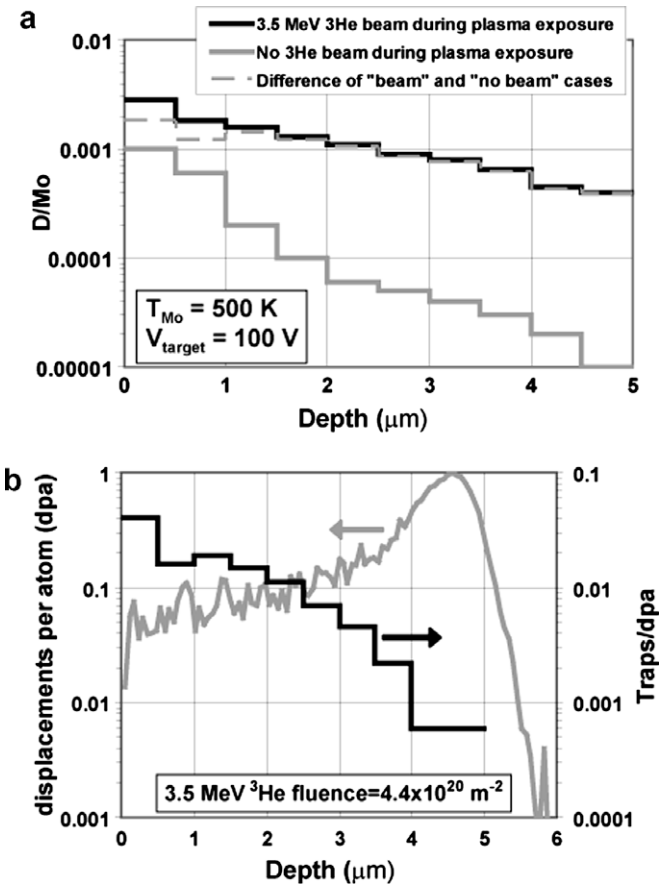

Fig. 5. (a) Comparison of D depth profiles with and without the ^{3}He ion beam present to a plasma fluence of 1.5×10^{24} D/m^2 and an ion beam fluence of 4.4×10^{20} ^{3}He/m^2. (b) The damage distribution (dpa) and ^{3}He ion implantation range for the exposure with the ^{3}He ion beam present. The traps/dpa curve is calculated from the difference from the curves in (a) and dividing by dpa curve in (b).

the deuterium concentration is non-zero at the end of detection range (5 μm) for intermediate (400–500 K) and high temperatures (600–700 K), it is possible there is deuterium trapped deeper than 5 μm in the Mo, meaning the retention values shown in Fig. 3(a) would be minimum retention values for these temperatures. This would imply that the lowest retention occurs at 300 K, which is counter to previous results [2,3].

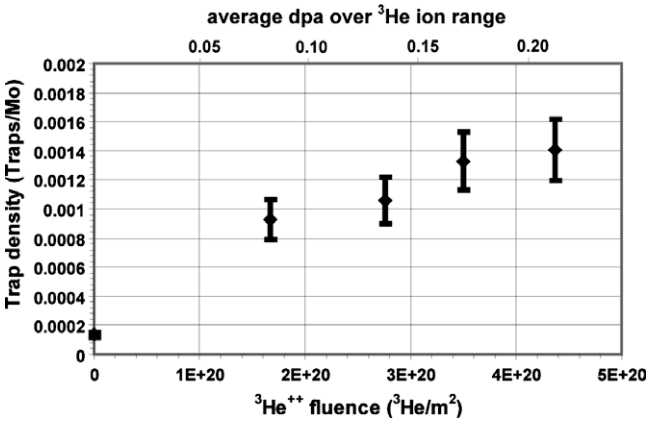

Fig. 6. The trap density in the first 5 μm of the Mo surface, as measured by NRA detection of trapped D atoms, as a function of the total 3.5 MeV ^{3}He^{++} fluence. Measurements were taken at T_{Mo} = 500 K and V_{bias} = 100 V. The zero and maximum (4.4×10^{20} ^{3}He/m^2) ^{3}He fluence cases correspond to the curves in Fig. 5(b).

TRIM [12] simulations show that at a 350 V target bias, incident D ions begin to create atomic displacements in Mo (assuming a 30 eV lattice binding energy). At target biases of 100 V, common plasma impurities such as carbon and oxygen are capable of creating displacements in the Mo surface although D ions cannot. At target biases below 50 V, neither the D ions nor plasma impurities are capable of creating displacements in the Mo lattice. Since the D retention is approximately equivalent for all these target biases, it follows that vacancies caused by the primary knock-ons of plasma ions are not a dominant trap source in the Mo for these experiments. The lack of retention-dependence on target bias also demonstrates that retention is weakly driven by the implantation range of the plasma ions.

3.2. Dynamics and role of diffusion in D retention

The depth profiles show that diffusion is playing an important role at lower T. The 300 K profile (Fig. 3(b)) appears to be diffusion-limited, but show D concentrations near the surface on the order of 1 at.% (i.e. much higher than any intrinsic trap density or hydrogenic solubility for Mo at low ambient pressure). The 400 K and 500 K profiles show a deuterium gradient away from the surface and the D begins populating trap sites deep (>4 μm) in the material. Exploiting the unique DIONISOS ability to measure the time evolution of the D depth profile, at 400 K we can see a "leading edge" of implanted D diffusing deeper into the bulk as the plasma exposure proceeds (Fig. 4). At the end of the 1500 s plasma exposure, the implanted D has just reached the end of the ^{3}He ion range (5 μm). This is consistent with calculations using the diffusion rate from Tanabe [13], which shows that diffusion across 5 μm in 1500 s is possible for $T_{Mo} \geqslant 400$ K and that the retention in the 300 K case is diffusion-limited.

It is also important to understand the state of the D in the Mo, in particular the energy wells in which they reside (e.g. shallow wells <0.5 eV are effectively mobile or solute at 300 K and above, while D in deep wells (>1.4 eV) are "trapped" and immobile). By measuring the time-dependence of D concentration and how it reacts to changing conditions this can help us distinguish the trapped (static) D from the solute/mobile (dynamic) D.

3.3. Trap production from irradiating 3.5 MeV ^{3}He ion beam

Ion beam analysis, such as NRA, is typically considered as a non-perturbing diagnostic and this is usually true for the case of post-mortem analysis where beam fluence is small with large detector solid angles. However, in a dynamic experiment, such as DIONISOS, where NRA is occurring during the plasma discharge, the ion beam is not only a diagnostic, but also a potential cause of damage in the material. A set of exposures was performed to further investigate this effect. For these tests a new Mo specimen was used for each exposure to the ^{3}He beam and plasma as opposed to the data acquired in Fig. 3 where the Mo targets were re-used after thermal desorptions.

The clearest indication of the influence of the ^{3}He analyzing beam can be seen in Fig. 5(a), where the final retention in the first 5 μm of the surface is much greater when the ion beam is present during the entire plasma exposure, rather than a "plasma only" exposure. Evidently a fraction of the Mo lattice atom displacements caused by the irradiating high-energy ^{3}He ions are converted into permanent lattice defect sites (i.e. vacancies, dislocations, voids) where hydrogenic isotopes can be trapped and stored [14–16]. In addition the implanted D from the plasma can adequately diffuse to these sites in order to "fill" traps at this target temperature (see Section 3.2). What remains an open question is how significant the contribution from displacement-produced trap sites is with respect to the overall retention properties of the Mo. From Fig. 5(a), the total retention in the first 5 μm of the surface for the He^3-irradiated target is 3.9×10^{22} D/m^2 and for the un-irradiated target is 0.44×10^{22} D/m^2. Thus, the displacement-induced trap sites are the dominant trap source in these experiments, contributing ~85% of the total trap sites in the Mo for the conditions in Fig. 5. A conversion rate for dpa to trap concentration can be estimated by taking the difference between the two curves in Fig. 5(a) to isolate the contribution by the ^{3}He irradiation and then relating this to the dpa profile determined by SRIM [12] (using 30 eV displacement energy for Mo) (Fig. 5(b)). This conversion rate is highest at the surface despite this being a region of relatively low total damage. In fact the D/Mo profile does not have any indication of enhancement near the ^{3}He end of range perhaps indicating a synergistic effect between the implanted D from plasma exposure and the ^{3}He irradiation-produced displacements, and certainly a complicated, likely non-linear, relationship between dpas and traps.

This motivates us to examine explicitly the scaling relationship between average dpa and trap concentration. In these experiments, Mo targets (new target used for each exposure) were exposed to identical plasma and surface conditions ($\Gamma_D = 1 \times 10^{21}$ D/m^2 s, $V_{bias} = 100$ V, $T_{Mo} = 500$ K, $\Phi_D = 1.5 \times 10^{24}$ D/m^2) but increasing 3.5 MeV ^{3}He fluences by varying the ion beam current irradiating the target during the plasma exposure. Fig. 6 shows the trap concentration integrated over the first 5 μm of the surface as a function of 3.5 MeV ^{3}He fluence. The dependence of trap density on ^{3}He fluence (and thus dpa level) scales in a less than linear fashion and can be qualitatively fit to a scaling $(\text{dpa})^{\alpha}$, where $\alpha = 0.25$–0.5.

3.4. Dynamic retention and D release

The surface release rate of hydrogenic species is of crucial importance in understanding how hydrogenic retention in the walls of long-pulse and steady-state fusion devices will evolve. Although the depth resolution is limited with NRA to ~500 nm, DIONISOS allows us to diagnose the time-dependence of the D concentration in the surface region, with and without the plasma driving permeation. This allows us to examine the relative quantities of D residing in shallow (solute) and deep (trapped) energy sites. Similar techniques of using NRA to determine near-surface solute concentrations have been used with neutral gas experiments [17].

On implantation from the plasma, the deuterium release from a surface, Γ_{out}, can be rate-limited by two processes: diffusion or surface recombination. In the case of diffusion the efflux is limited by the diffusivity, d, and near-surface solute density, $n_{D,0}$, gradient from the implantation depth, δ, back to the surface, i.e. $\Gamma_{out} < d\, n_{D,0}/\delta$. In the second case recombination of two atomic D into volatile D_2 at the surface limits the D release, i.e. $\Gamma_{out} < 0.5\ n_{D,0}^2\ R$ where R (m^4/s) is the recombination coefficient.

The DIONISOS system has been utilized to determine $n_{D,0}$, thus providing insight into the rate-limiting surface-efflux mechanism. Once the plasma is removed the concentration of near-surface solute D, $n_{D,0}$, will return to the natural solubility levels of the material (<1 appm for Mo at this T and ambient gas pressure) and the trapped D, by definition, will remain unchanged. Therefore, the approximate measurement of $n_{D,0}$ is the immediate (within time resolution of NRA) decrease in the total (solute + trapped D) measured density in the top surface slab back to the trapped D concentration only. We denote this measured density decrease $\Delta n_{D,surf}$. An example of such a measurement is found in Fig. 7(a) where $\Delta n_{D,surf}$ is clearly determined. The compilation of $\Delta n_{D,surf}$ for different exposure conditions is shown in Fig. 7(b).

There is a clear decrease in $\Delta n_{D,surf}$ with increasing target bias. If the release of D from the surface was diffusion-limited one would expect to see $\Delta n_{D,surf}$ *increase* with increasing implantation depth (higher D^+ energies), since the diffusivity and incident flux are con-

stant. However the experimental trend is the opposite. An additional characteristic of the data, consistent with recombination as the rate-limiting process for surface loss, is that the $\Delta n_{D,surf}$ values organize well to an Arrhenius relationship, One does not expect a direct dependence of R on incident ion energy. However we believe this is a result of the higher energy D ions inducing more sputter cleaning of the surface; cleaned Mo surfaces in general have increased recombination rates [18,19].

Under the assumption that recombination is the rate-limiting process for surface loss we can infer an effective surface recombination coefficient, R, through the equilibrium condition of $\Gamma_{out} = \Gamma_{in}$; so $\Gamma_{D+,in} = 0.5\ \Gamma_{D2,out} = 0.5\ (n_{D,0})^2 R = 0.5\ (\Delta n_{D,surf})^2 R$. Our inferred R values (Fig. 7(b) right-hand axis) are at the lower end of surface recombination coefficients measured for tungsten [20,21] and much lower than those predicted by theory [22]. Part of this discrepancy can be explained by the non-ideal surface of the Mo targets. Contrary to other recombination studies where the surface is sputter-cleaned and annealed [17–20], our targets underwent no special preparations of the surface (rough, un-annealed, etc.). While this makes it more difficult to compare the R values to theory, it more closely resembles the conditions inside a tokamak where low-Z surface impurities are ubiquitous.

We note that the inferred R values in this study can only be considered an effective surface recombination coefficient in the sense that it is the limiting factor of the release of D from the surface. Since we are limited to a depth resolution of 500 nm, other processes may be included in this R value that are not considered in theory or more carefully factored out in more precise experiments. Regardless of the interpretation, the important insight is that the near-surface solute (mobile) D concentrations are significantly enhanced compared to intrinsic solution expectations, and measuring this directly gains important insights into the physical processes at play.

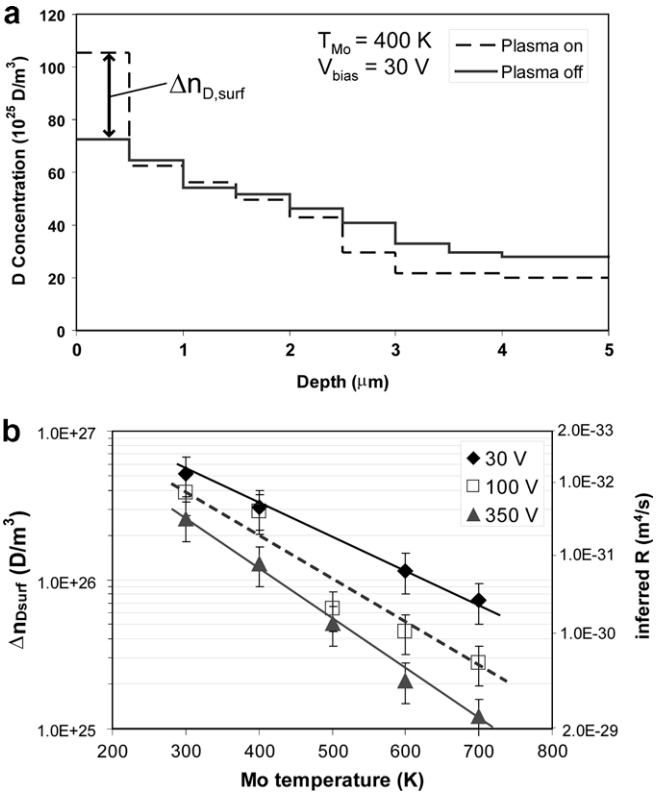

Fig. 7. (a) The D depth profile immediately before and after the plasma is turned off demonstrating how $\Delta n_{D,surf}$ is determined, and (b) The $\Delta n_{D,surf}$ values for all exposures in Fig. 3 and the corresponding inferred surface recombination coefficient (R).

4. Discussion

The absence of a peak in the retention at the end of the ^{3}He ion range, where the ^{3}He irradiation damage is concentrated is probably related to a number of factors. The non-linear relationship between trap concentration and dpa (Fig. 6) will help to "flatten" the distribution of traps created by ^{3}He irradiation. At 300 K, we know the implanted D cannot diffuse into the material far enough in a 1500 s exposure to reach the deep (>3 μm) trap sites produced by the ^{3}He irradiation. At 400 K, the leading edge of the deuterium is just reaching the end of the ion range after 1500 s, so the deep trap sites are just beginning to fill (Fig. 4). At the higher temperatures, where the implanted D has greater access to the ^{3}He irradiation traps, other effects may be activated, such as higher rates of trap annealing or trap diffusion. Certainly the diffusion/mobility of traps would help flatten any peaks in the trap distribution. Also, as vacancies become mobile at higher temperatures, they are more likely to encounter a grain boundary or interstitial atom and repair themselves thereby removing a potential trap site from the lattice.

The peaked retention at the surface could be explained by several effects. Since the Mo targets are un-annealed, it is possible there is a large concentration of inherent traps at the surface due to fabrication and machining stresses. However, if this were the case, one would expect the D concentration in the near-surface to be the same for all exposures, but the data shows the D retention near the surface decreases with increasing temperature (Fig. 3(b)). This could be explained if these inherent trap sites had a low trapping energy. Another possible explanation of peaked retention at the surface is that the plasma implantation is producing trap sites. Studies in tungsten have shown that exposure of materials with low solubility to high plasma fluxes can "super-saturate" the material and produce stresses in the lattice that are relieved through the production of dislocations and vacancies [23–25]. Connecting trap production to plasma flux could also be part of the explanation as to why the retention in the 100 V exposures is the same as the 30 and 350 V exposures despite receiving less ^{3}He fluence. It is also possible that the simultaneous implantation of D with the He^3 damage may have a synergistic effect; the D could be filling vacancies making it harder for them to recombine with interstitials or annihilate at grain boundaries. This could lead to a significant enhancement of trap production in the near-surface where the implanted D atoms have more immediate access to the traps.

5. Conclusions

The unique capability of DIONISOS to dynamically measure D retention allows for these first experimental measurements of deuterium release rates during and after a plasma exposure. From these release rates an "effective" surface recombination coefficient can be inferred. The inferred values are lower that those predicted by theory and measured for tungsten. This might be expected given the unprepared nature of the Mo surfaces (i.e. dirty, rough, etc.) and the fact that poor depth resolution means other processes may be included in these values rather than a pure measurement of surface recombination. However, the release rate from impure, unprepared surfaces will be critical to understanding fuel retention in the walls of ITER and other long-pulse or steady-state fusion devices.

The unique conditions produced in the DIONISOS experiment have also yielded important insights into the behaviour of hydrogenic retention in Mo in a nuclear environment. Irradiation with MeV-energy particles leads to significant enhancement of trap

densities spread throughout the measurement range. At elevated temperatures, $T_{Mo} > 500$ K, implanted D from the plasma can access these traps, which results in significant retention distributed throughout the entire ^{3}He ion range. At this time we cannot with certainty determine the absolute contributions of the various effects of solute D diffusivity, trap migration, and trap annealing/annihilation. It is our interpretation that the conditions for highest retention appear to be a Mo target of intermediate temperature (400–500 K) exposed to a high fluence of MeV irradiating ions as this maximizes retention by allowing the implanted D to populate the MeV ion-produced trap sites. Certainly one would expect at the higher temperatures (700 K) thermal de-trapping and trap annealing can begin to play a role and overall retention can begin to decrease. Operation at much higher temperatures (>700 K) would appear to help alleviate hydrogenic retention concerns even in a neutron environment. Clearly more research on retention behaviour in a nuclear environment is needed as the presence of MeV ions (or neutrons) appears to be a dominant factor for retention in high-Z materials.

Acknowledgements

This work was supported by US Department of Energy Plasma Physics Junior Faculty Development award, DE-FG02-03ER54727 and US Department of Energy award, DE-FC02-99ER54512.

References

[1] S. Nagata, T. Hasunuma, K. Takahiro, S. Yamaguchi, J. Nucl. Mater. 248 (1997) 9.
[2] A.A. Haasz, J.W. Davis, J. Nucl. Mater. 241–243 (1997) 1076.
[3] K.L. Wilson, A.E. Pontau, J. Nucl. Mater. 85&86 (1979) 989.
[4] R.A. Causey, C.L. Kunz, D.F. Cowgill, J. Nucl. Mater. 337–339 (2005) 600.
[5] R. Sakamoto, T. Muroga, N. Yoshida, J. Nucl. Mater. 233–237 (1996) 776.
[6] B. Lipschultz, Y. Lin, M.L. Reinke, D. Whyte, A. Hubbard, I.H. Hutchinson, J. Irby, B. LaBombard, E.S. Marmar, K. Marr, J.L. Terry, S.M. Wolfe, The Alcator C-Mod Group, Phys. Plasmas 13 (2006) 056117.
[7] D.G. Whyte, B. Lipschultz, G.M. Wright, J. Irby, R. Granetz, B. LaBombard, J. Terry, Proceedings of the 21st IAEA Fusion Energy Conference, Chengdu, China, 2006.
[8] G.M. Wright, D.G. Whyte, B. Lipschultz, R.P. Doerner, J.G. Kulpin, J. Nucl. Mater. 363–365 (2007) 977.
[9] V.Kh. Alimov, M. Mayer, J. Roth, Nucl. Instr. and Meth. B 234 (2005) 169.
[10] M. Mayer, Technical Report IPP 9/113, Max-Planck-Institut für Plasmaphysik, Garching, Germany, 1997.
[11] M. Mayer, Proceedings of the 15th International Conference on the Application of Accelerators in Research and Industry, American Institute of Physics Conference Proceedings 475 (1999) 541.
[12] J.P. Biersack, L. Haggmark, Nucl. Instr. and Meth. 174 (1980) 257.
[13] T. Tanabe, Y. Furuyama, N. Saitoh, S. Imoto, Trans. Jap. Inst. Met. 28 (1987) 706.
[14] T. Hyodo, B.T.A. McKee, A.T. Stewart, Radiat. Eff. Lett. 68 (1982) 77.
[15] S.V. Naidu, A. Sen Gupta, R. Roy, P. Sen, Positron Annihilation, in: Proceedings of 7th International Conference, 1985, p. 476.
[16] I. Takagi, S. Watanabe, S. Nagaoka, K. Higashi, Fusion Science and Technology 41 (2002) 897.
[17] W.R. Wampler, P.M. Richards, Phys. Rev. B 41 (1990) 7483.
[18] W.R. Wampler, J. Appl. Phys. 65 (1987) 4040.
[19] W.R. Wampler, J. Vac. Sci. and Technol. A 9 (1991) 1334.
[20] R.A. Anderl, D.F. Holland, G.R. Longhurst, R.J. Pawelko, C.L. Trybus, C.H. Sellers, Fus. Technol. 21 (1992) 745.
[21] P. Franzen, C. Garcia-Rosales, H. Plank, V.Kh. Alimov, J. Nucl. Mater. 241–243 (1997) 1082.
[22] M.A. Pick, K. Sonnenberg, J. Nucl. Mater. 131 (1985) 208.
[23] M. Poon, R.G. Macaulay-Newcombe, J.W. Davis, A.A. Haasz, J. Nucl. Mater. 307–311 (2002) 723.
[24] V.Kh. Alimov, K. Ertl, J. Roth, J. Nucl. Mater. 290–293 (2001) 293.
[25] O.V. Ogorodnikova, J. Roth, M. Mayer, J. Nucl. Mater. 313–316 (2003) 469.